Amide Spacing Influences pDNA Binding of Poly(amidoamine)s

ARTICLE *in* BIOMACROMOLECULES · FEBRUARY 2010

Impact Factor: 5.75 · DOI: 10.1021/bm900824g · Source: PubMed

3 AUTHORS, INCLUDING:

Lisa Prevette
University of St. Thomas
10 PUBLICATIONS **389** CITATIONS

Amide Spacing Influences pDNA Binding of Poly(amidoamine)s

Lisa E. Prevette,[†] Matthew L. Lynch,[‡] and Theresa M. Reineke*[,†,§]

Department of Chemistry, University of Cincinnati, P.O. Box 210172, Cincinnati, Ohio 45221-0172, The Procter & Gamble Company, Corporate Research Division, Miami Valley Laboratories, 11810 East Miami River Road, Cincinnati, Ohio 45252-1038, and Department of Chemistry and Macromolecules and Interfaces Institute, Virginia Tech, Blacksburg, Virginia 24061

Received July 20, 2009; Revised Manuscript Received October 10, 2009

Previously, a series of three poly(amidoamine)s was designed and synthesized by polymerizing oxylate, succinate, or adipate groups with pentaethylenehexamine. These resulting polymers (named **O4**, **S4**, and **A4**, respectively) were created as models to poly(glycoamidoamine) nucleic acid delivery agents to understand how the absence of hydroxyl groups and changes in the amide bond spacing affect polymer degradation, plasmid DNA (pDNA) encapsulation, toxicity, and transfection efficiency in vitro. To understand differences in the biological properties quantitatively, we investigated the mechanism of interaction between these macromolecules and pDNA to reveal differences in pDNA binding affinity and complexation as a function of structure. Herein, several analytical techniques such as dynamic light scattering, circular dichroism, thermal gravimetric analysis, isothermal titration calorimetry (ITC), and ethidium bromide exclusion assays were used to examine the pDNA binding strength of **O4**, **S4**, and **A4**, and the results are compared with the previous series of poly(glycoamidoamine)s. It was found that the length of the amide bond spacer in these nonhydroxylated analogs did affect the pDNA binding affinity to a small degree (binding affinity order **A4** > **S4** > **O4**). The increase in binding affinity with longer methylene spacer was not due to hydrophobic interactions but likely from optimization in electrostatic interactions and hydrogen bond formation. Even though **O4** was revealed to have the lowest pDNA binding affinity of the nonhydroxylated series, this polymer yields the highest cellular transfection efficiency, which is likely an effect of the faster hydrolysis rate.

Introduction

Polycations capable of binding and condensing nucleic acids into nanoparticle complexes termed "polyplexes" are being widely studied to enhance the cellular delivery of polynucleotides for medical research and therapeutic development. The ability of these agents to transfect cells with polynucleotides efficiently without causing a toxic response has been shown to be highly dependent upon their structure (i.e., molecular weight,[1] charge density,[2,3] and hydrophobicity[4]). Previously, we have shown that poly(glycoamidoamine)s (PGAAs), designed and synthesized in our lab (**G4**, **D4**, **M4** and **T4**; Figure 1a), have been revealed to be outstanding nucleic acid delivery agents, and subtle changes in their structure (i.e., stereochemistry of the hydroxyls within the repeat unit) play a role in delivery efficacy.[5,6] Our studies have revealed that these structures have different affinities for complexing plasmid DNA (pDNA) to form polyplexes, and the binding properties are dependent upon the stereochemistry of the carbohydrate hydroxyl groups in the repeat unit.[6,7] Through a number of biophysical characterization methods, it was concluded that in addition to electrostatic interactions between the protonated amines on the polymer and the phosphate groups on the pDNA backbone, the polymer hydroxyl and uncharged amine groups were participating in hydrogen bonding (likely to the pDNA base pairs), which stabilizes pDNA encapsulation.[7]

It was also noticed that these PGAA polyamides appeared to hydrolyze rapidly under mild aqueous conditions, and it was hypothesized that the functional groups (both the hydroxyls and amines) synergistically facilitate degradation. This property could be aiding pDNA release and enhancing reporter gene expression. As shown previously,[8] our data revealed that this was the case. Structures that contain hydroxyls (**G4**, **D4**, **M4**, **T4**) readily degrade, and higher gene expression is observed in transfection experiments. When these degradable PGAA vehicles were compared with analogous polymers that retain similar spacing between the amides but lack the hydroxyl units (Figure 1b; **O4, S4, A4**), the nonhydroxylated structures (**A4** and **S4**) did not readily degrade under aqueous conditions at physiological temperature. In turn, lower reporter gene expression was also found with these polymeric vehicles in transfection experiments. Yet, when **O4** was examined, it was found that this polymer degraded under these conditions, and higher gene expression was also found. These data indicate that the pDNA binding affinity, degradation, and release profiles all play a role in enhancing transfection efficiency.

Although degradation could certainly affect the release of nucleic acid cargo in the cell and thus promote transcription and translation of genes, there may be other factors governing the unpackaging of nucleic acids from the vehicle, which would manifest itself as a variation in transfection efficiency. For example, amide spacing, the lack of hydroxyls, and polymer hydrolysis could influence pDNA binding affinity to a large degree. Knowledge of the strength and mechanism of interaction between these macromolecules and pDNA can aid in our understanding of the cause of differences in biological activity and the design of improved structures. Toward this end, isothermal titration calorimetry (ITC), dynamic light scattering, and ethidium bromide (EB) exclusion assays were completed to determine pDNA association constants for each of the three

* To whom correspondence should be addressed. E-mail: treineke@vt.edu.
[†] University of Cincinnati.
[‡] The Procter & Gamble Company.
[§] Virginia Tech.

10.1021/bm900824g
Published on Web 01/08/2010

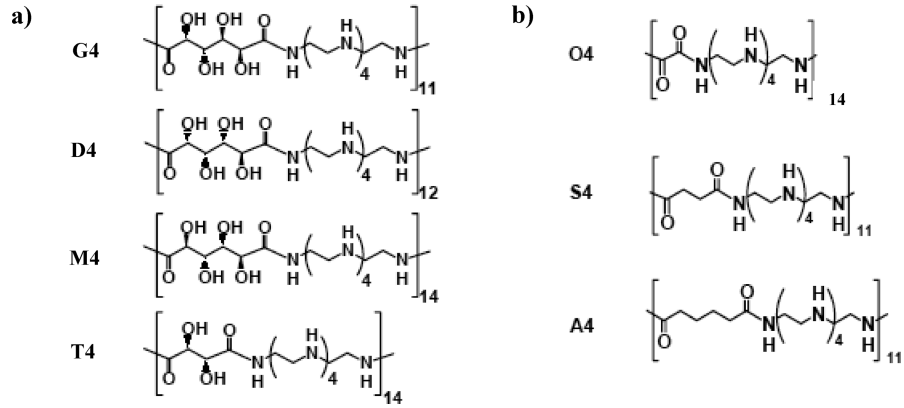

Figure 1. Structures of (a) the poly(glycoamidoamine)s (PGAAs) studied previously (some branching of the polymer structure is present off of the secondary amines)[5−7] and (b) the hydroxyl-free poly(amidoamine) (PAA) analogues.[8]

poly(amidoamine) (or PAA) analogs. Indeed, differences in chemical structure (amide spacing and the absence of hydroxyl groups within the polymer) were demonstrated to affect the binding affinity. Circular dichroism spectra revealed noticeable pDNA secondary structure changes upon the addition of high molar ratios of PAA. Such a transition suggests direct interaction of the polymers with the base pairs, possibly through amide and amine hydrogen bonding, and this interaction was enhanced by a longer methylene spacer. Amide linkages are known to be involved in hydrogen bonding to the nitrogenous bases of DNA.[9−11] In comparing these agents to the analogous PGAAs, pDNA binding strength remained significant with the removal of the carbohydrate hydroxyl groups, demonstrating that hydrogen bonding from these regions is not necessary for strong pDNA association. However, the presence of these functionalities appears to alter the mechanism of interaction between the polymer and nucleic acid.

Materials and Methods

All data are reported as the average of at least three trials using separately prepared polymer and pDNA samples.

Materials. Tris (Aldrich; Milwaukee, WI) and EB (Sigma; St. Louis, MO) were used as received. The pCMV-β technical grade pDNA was purchased from PlasmidFactory (Bielefeld, Germany) and dialyzed extensively into buffer. Tris buffer was prepared to 10 mM using Millipore (18 Ω) water and titrated to proper pH using HCl (Acros; Morris Plain, NJ). The polycations were synthesized and characterized as described previously[8] with molecular weight (M_w), degree of polymerization (dp), polydispersity index (M_w/M_n), and the Mark−Houwink−Sakurada (MHS) α parameter listed in Table 1.

Dynamic Light Scattering. Polyplex hydrodynamic diameter was measured at increasing N/P ratio [ratio of the amine groups (N) in the polymer to phosphate groups (P) in the pDNA used for formulation of the polyplexes] by titrating 1.46 mL of 0.31 mM pDNA solution in 10 mM Tris buffer pH 7.4 with 20 μL aliquots of 5.5 mM PAA solution in the same buffer, using a NanoSeries Zetasizer ZS (Malvern; Worcestershire, U.K.). The instrument employs a 4.0 mW He−Ne laser operating at 633 nm with a 173° scattering angle. Correlation functions were analyzed using z-average cumulant fit of the data with an average of three runs of three measurements, each after thorough mixing of each sample and a 5 min equilibration time.

Isothermal Titration Calorimetry. A 1.46 mL solution of 0.31 mM pDNA in 10 mM Tris buffer pH 7.4 was titrated with 10 μL aliquots of 5.5 mM PAA solution in the same buffer at 25 °C using a Microcal VP-ITC (Northampton, MA). These concentrations were selected on the basis of obtaining enough signal and ensuring saturation of the binding sites at an optimal titration point to observe the full binding curve. The injections were spaced 200 s apart with a reference power of 10. The pDNA was dialyzed extensively against buffer, and the resulting dialysate was used to prepare the polymer sample to reduce pH and ionic strength differential artifacts upon titration. pDNA concentration was quantified after dialysis using the absorbance band at 260 nm, with 1 au = 50 μg/mL pDNA. All samples were degassed prior to use. The data was fit to a standard one-site model using Origin 7.0 software, with the enthalpy (ΔH_{obsd}), binding constant (K_{obsd}), and stoichiometry (n) as free-floating parameters. For the heat capacity study of **A4**-pDNA binding, the same experimental settings and concentrations were used; however, the temperature was changed (from 20 (293 K) to 40 °C (313 K)) during each run.

Ethidium Bromide Exclusion Assay. The fluorescence of EB upon intercalation with pDNA (and subsequent decrease upon EB exclusion via PAA binding) was used to compare the relative pDNA binding affinities of the polymers according to the method of Read et al.[12] Fluorescence measurements were acquired using a Varian Cary spectrofluorometer with λ_{ex} = 510 nm, λ_{em} = 590 nm, slit width = 10 nm, and an integration time of 3 s. All solutions were made in 10 mM Tris pH 7.4 buffer. The fluorescence of a 400 ng/mL EB solution (F_{bg}) and a 10 μg/mL solution of pDNA containing 400 ng/mL of EB (F_{DNA}) were first measured as controls. We completed EB exclusion assays with each polymer and pDNA by titrating 2.0 mL of the F_{DNA} solution with each polymer at 0.5 N/P ratio aliquots (50 μL of a 26 μg/mL polymer solution). After the addition of each 50 μL polymer aliquot, the solution was gently mixed and the reduction in fluorescence (F_x) was measured. The percent relative fluorescence ($\%F$) was determined using the equation below

$$\%F = 100\frac{F_x - F_{bg}}{F_{DNA} - F_{bg}}$$

Circular Dichroism. Circular dichroism spectra were obtained using a Jasco J-715 spectropolarimeter as an average of three iterations at 25 °C. A 1.46 mL solution of 0.31 mM pDNA in 10 mM Tris pH 7.4 buffer was titrated with various amounts of 5.5 mM PAA solution to reach polymer amine (N)/DNA phosphate (P) ratios of 0−5. These concentrations and titration volumes were used to mimic those of the ITC experiment. A scan rate of 50 nm/min, a resolution of 0.5 nm, and wavelengths from 225−350 nm were chosen.

Thermal Gravimetric Analysis. Samples of 1.0 mg of each polymer were slowly heated from 25 to 900 °C using a Netzsch TGA/DSC (Burlington, MA) and the mass measured at 0.5 °C increments.

Results and Discussion

Dynamic Light Scattering. The intensity-averaged hydrodynamic diameter of polyplexes in Tris buffer was measured to identify the presence of micrometer-scale aggregate formation

Table 1. Physical Characteristics of Poly(amidoamine)s Used Herein: Molecular Weight (M_w), Degree of Polymerization (dp), Polydispersity Index (M_w/M_n), and Mark−Houwink−Sakurada Parameter (α)[8]

polymer	M_w (kDa)	dp	M_w/M_n	α
A4	3.8	11	1.1	0.69
S4	3.5	11	1.1	0.71
O4	4.0	14	1.2	0.69

due to van der Waals interactions between the nanoparticles. This information is crucial to understanding the larger-scale events governing the association of these polycations with pDNA at many N/P ratios and for the proper analysis of the microcalorimetry data. It should be mentioned that the heat contributions related to polyplex aggregation are typically removed from the ITC data prior to curve fitting (vide infra). pDNA-only (N/P = 0) measurement was not included (Figure 2) because of the inaccuracy of fitting the correlation function of a nonspherical particle (i.e., molecular tumbling or barrel rolling could be contributing to the correlation function because plasmid DNA possesses plectonemic supercoil tertiary structure in solution,[13,14] providing it rodlike character). This is usually seen as the presence of a second or third decay on earlier time scales, which was witnessed in all of our pDNA-only trials; this inaccurate data corresponded to an average pDNA diameter of ∼25 nm (data not shown).

As shown in Figure 2, **A4** and **O4** polyplex size remained fairly constant from N/P = 0.24 to 2.2, after which point aggregation was induced as a result of pDNA phosphate charge neutralization by binding polycation (ζ potential of free pDNA is −43 mV and became less negative with increasing polymer ratio, reaching 0 mV by N/P = 5, data not shown). This point of aggregation onset was delayed until N/P = 2.7 for **S4**, which could be related to the spacing of the amide and amine groups, the solution structure of these macromolecules, or both. The ability of these PAAs to neutralize pDNA phosphate charge and cause flocculation is an indirect indication of the macroscopic binding event and thus overall pDNA binding affinity. Therefore, these results suggest that the length of the amide spacer influences, to a small extent, this important property.

pDNA Binding Affinity. To investigate quantitatively the pDNA binding affinity of **A4**, **S4**, and **O4** and compare the results with those of the previous PGAA structures, microcalorimetry was performed to obtain binding constants, enthalpy, entropy, and the stoichiometry of their interaction.[15] The addition of small aliquots of polymer to a dilute solution of pDNA in an adiabatic cell translated into heat changes per injection, Q. These heats could be related to the enthalpy (ΔH) and stoichiometry of the interaction (n), using M as the concentration of macromolecule, V as the volume of the cell, and Θ as the fraction of ligand bound to the macromolecule by fit to a standard one-site model

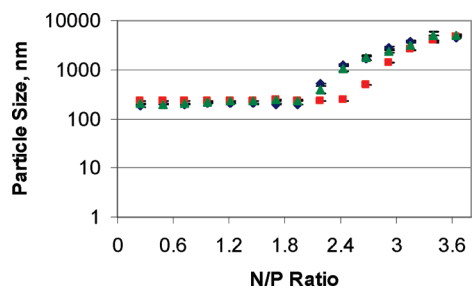

Figure 2. Polyplex size of 0.31 mM pDNA and 5.5 mM PAA at 25 °C upon increasing molar ratio of **A4** ◆, **S4** ■, and **O4** ▲.

$$Q = MVn\Theta\Delta H$$

One can solve for Θ by using the equilibrium equation for the binding constant K, with X as the concentration of ligand and [X] as the free ligand concentration

$$K = \frac{\Theta}{(1 - \Theta)[X]} \quad \text{and} \quad [\mathrm{X}] = X - Mn\Theta$$

It is critical to subtract extraneous contributions to the heat signal, such as dilution of both macromolecules and aggregation phenomena before attempting to fit the curve to a binding-only model. Dilution controls were performed for each polymer, and the magnitude of these heats differed with polymer structure (data not shown), leading to different thermogram shapes for the association of each polymer with pDNA, as shown in the top halves of Figure 3a,b,c. Once these dilution signals were subtracted from the raw data, the three pDNA binding isotherms were more uniform (bottom halves of Figures 3a,b,c).

Using the dynamic light scattering results herein, we were able to correlate roughly the point of aggregation onset to the injections on the thermogram, and we chose to delete these points before fitting the data (shown in the bottom sections of Figure 3). We chose to remove three extra injection points in the case of **S4** because an endothermic change, that we suspect is aggregation, occurred at N/P = 2.0. Differences in complex formation resulting from constant stirring in the ITC cell likely render differences in the points of aggregation between the DLS data (taken without stirring) and the isotherms, but our experience has shown that aggregation is an endothermic process, consistently observable in the thermograms.[7,16,17] Further evidence of this endothermic event corresponding to aggregation stems from the work of Alvarez-Lorenzo et al., where the micellization processes of Pluronic (PEO-PPO-PEO) polymers L92 and P123 were both accompanied by endothermic enthalpic changes.[18] The endothermic event occurring postsaturation may also derive from DNA collapse, as suggested by Matulis et al.[19] and Patel and Anchordoquy;[20] however, distinguishing between aggregation of polyplexes and DNA condensation is likely impossible because the events occur simultaneously. Either way, by eliminating the subsequent data points, we reduce the isotherm to a binding-only representation that can be properly fit with the Langmuir model.

The data were best fit by using a standard one-site model included on the Origin software, and we have attributed this binding to be due to a combination of charge−charge/electrostatic, van der Waals, and hydrogen bonding forces, as we anticipated each to play a role in this system containing secondary amines (both protonated and unprotonated) and amides. We showed in our previous paper on PGAA-pDNA binding mechanisms[7] that a nonelectrostatic interaction, most likely hydrogen bonding, was playing a role in the binding mechanism of all four hydroxylated polymers. Interestingly, a two-site binding model was necessary to fit the PGAA-pDNA binding isotherms, which we attributed to the strong presence of both long-range charge−charge and short-range hydrogen bonding interactions. The first, primarily electrostatic interaction was characterized by a binding constant K_1, and the second primarily hydrogen bonding interaction was characterized by K_2. Polymers **G4** and **T4** had the most significant contribution of H-bonding to the pDNA association, which could be due to their more favorable carbohydrate hydroxyl stereochemistry. It should be noted that the close fit of the PAA-pDNA binding isotherms to the one-site model suggests that H-bonding is a

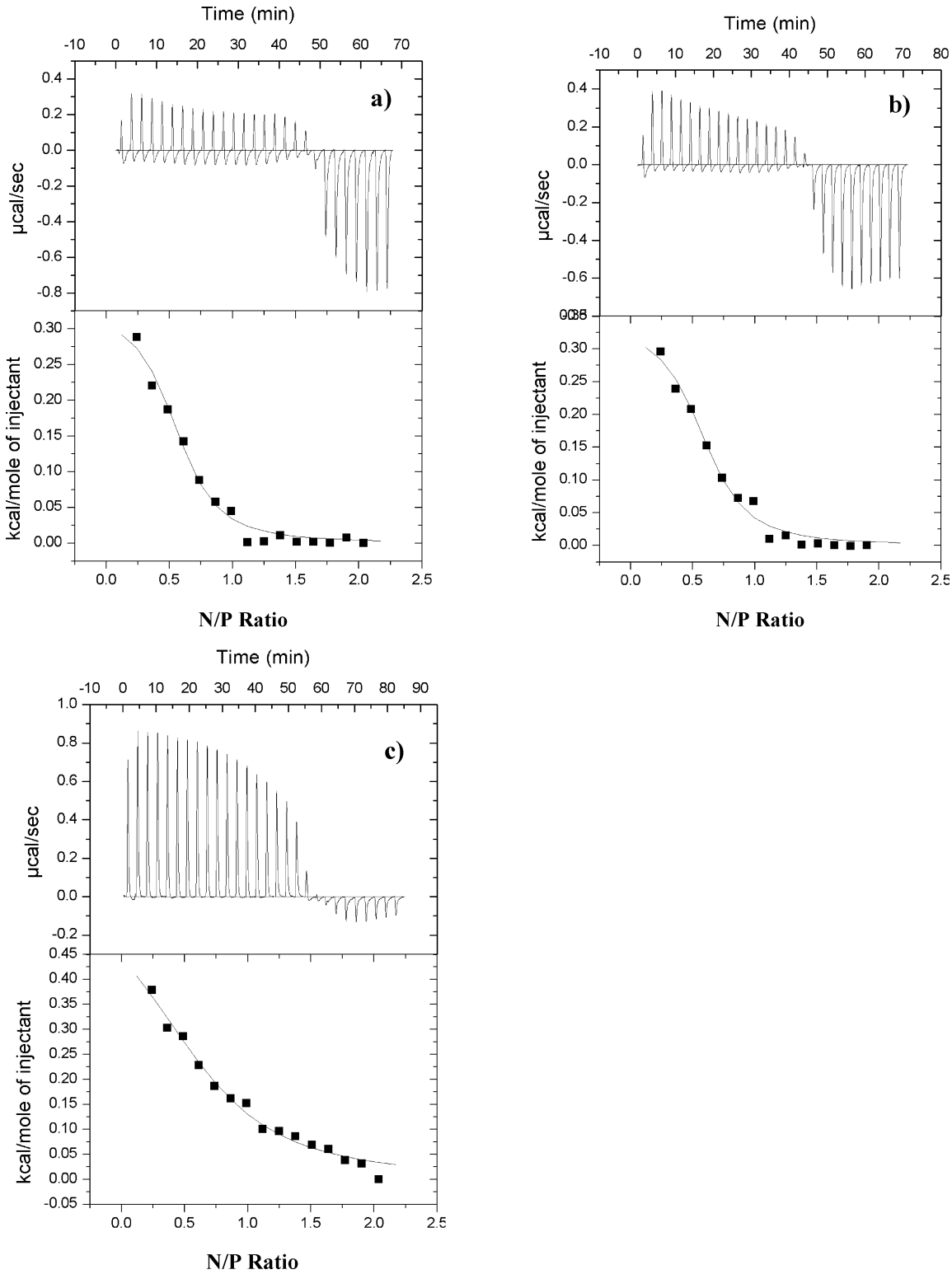

Figure 3. ITC thermograms of 5.5 mM (a) **A4**, (b) **S4**, and (c) **O4** titrated into 0.31 mM pDNA in 10 mM Tris pH 7.4 buffer at 25 °C. Raw heat per injection is shown on top, with normalized data and curve fit on bottom. Points containing aggregation heats (after N/P = 2.2 for **A4** and **O4** and after 1.8 for **S4**) were subtracted from the normalized data prior to curve fitting.

less significant force of pDNA interaction for these nonhydroxylated analogues compared with the PGAAs.

As shown in Table 2, the PAA-pDNA associations were very slightly endothermic, as were those of the PGAAs previously studied. This reflects a process driven by entropy via the release of counterions and solvent upon binding, as is common for cation−DNA interactions.[19,21,22] Binding constants were determined to be on the order of 10^4 M^{-1}, similar to other polymer

Table 2. Thermodynamic Parameters for the Interaction of the Poly(amidoamine)s with pDNA in 10 mM Tris pH 7.4 Buffer at 25 °C

	$K_1 \times 10^{-4}$, M^{-1}	ΔH_1, kcal/mol	ΔS_1, kcal/(mol K)	n_1
A4	7.9 ± 2.6	0.29 ± 0.05	0.023 ± 0.001	0.55 ± 0.02
S4	4.9 ± 1.0	0.33 ± 0.01	0.023 ± 0.001	0.57 ± 0.01
O4	1.2 ± 0.0	0.58 ± 0.04	0.021 ± 0.000	0.86 ± 0.31

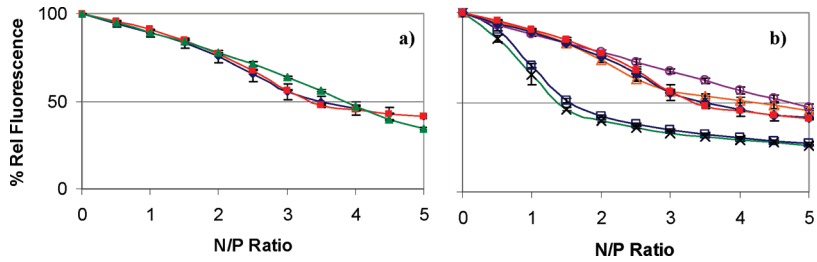

Figure 4. Reduction in fluorescence as a result of ethidium bromide exclusion from pDNA by various molar ratios of (a) **A4** blue ◆, **S4** red ■, and **O4** green ▲. (b) Results of **A4**- and **S4**-pDNA binding as compared with the analogous PGAAs **G4** blue □, **D4** orange △, **M4** purple ○, and **T4** green ×.

or protein nucleic acid associations.[20,23,24] These K values are also smaller than both K_1 and K_2 for **G4**, **D4**, and **T4** containing the carbohydrate hydroxyl moieties, which we suggested are forming polyplex-enhancing hydrogen bonds to the plasmid, depending on their stereochemistry. **M4**, the weakest pDNA binder of the PGAAs, was shown to have a K_2 value of 1.4×10^4 M^{-1}. Because we attributed the second binding interaction to the one with more hydrogen bonding contribution, this lower K_2 value suggests that the carbohydrate hydroxyl moieties of **M4** have less favorable stereochemistry. PAA-pDNA association constants were all also on this order (7.9×10^4 M^{-1} for **A4**, 4.9×10^4 M^{-1} for **S4**, and 1.2×10^4 M^{-1} for **O4**). Therefore, by removing the hydroxyl groups from the polymer structure in the analogous PAAs, it appears we have eliminated some complex-stabilizing hydrogen-bonding capability that was present for **G4**, **D4**, and **T4**. This result is obviously influential in our design of efficacious nucleic acid delivery vectors.

Next, we compared our ITC results with a commonly employed method for comparing the pDNA binding affinity of polymeric vectors based on the enhanced fluorescence of the ethidium molecule when intercalated in the double helix. Upon polymer binding to the nucleic acid, the ethidium is excluded, resulting in reduced fluorescence intensity. This fluorescence decrease can be qualitatively correlated to DNA binding affinity and is reported as an IC_{50} value (the N/P ratio of polymer necessary to inhibit 50% of the relative EB-DNA fluorescence). As shown in Figure 4, the three PAAs demonstrated different abilities to reduce the fluorescence of the DNA−ethidium complex. The IC_{50} value for **A4** and **S4** was 3.5, and **O4** possessed a similar value of 3.9 (possibly a result of its slightly weaker interaction with pDNA). Comparing this result with the ITC data, the qualitative nature of this assay is evident. Differences in the binding affinities of the PAAs with pDNA are not readily distinguishable in the EB assay results, whereas with microcalorimetry, we have shown that **A4** has a stronger association. Possible interactions between the polymers and the bases of the nucleic acid or the ethidium molecule itself may influence the dye displacement from its intercalated position in pDNA.

When this data is plotted concurrently with that of the analogous PGAAs studied previously[7] (Figure 4b), the influence of polymer structure on pDNA binding is clearly noticed. Here we show only results for **A4** and **S4** due to the analogous spacing of the amides. Interestingly, the PAAs behaved similarly to the weaker pDNA-binding PGAAs, **D4** and **M4**. These data supported our previous ITC data that indicated that **D4** and **M4** have a lower H-bonding contribution to their pDNA binding and appear to interact primarily through electrostatics. The EB assays, coupled to the ITC results, suggest that the hydroxyl stereochemistry, rather than their presence or absence, determines the strength and mode of pDNA binding. The pDNA binding affinities measured via ITC and EB exclusion assay suggest that binding strength may play a role in the biological properties of these vectors, along with other factors. For example, in the case of the degradable PGAAs, stronger pDNA association constituted higher transfection efficiency. However, with the hydroxyl-free PAAs, the degradable **O4** yielded the highest gene expression. Whereas **A4** and **S4** appear to have very similar structure and properties, **A4** (with slightly higher pDNA binding affinity) was shown previously to have higher cellular uptake, gene expression, and cell viability.[8] While we do not currently understand this difference, certainly intracellular trafficking can also play a large role in delivery efficacy.

Binding-Induced pDNA Secondary Structure Changes. The interaction of the PAAs with pDNA can also be monitored through changes in the DNA circular dichroism[25] spectra upon increasing N/P ratio. CD spectra allow us to observe changes in the pDNA secondary structure upon polymer binding. Because there are no CD spectral features of the polymers above 230 nm, the spectra here can be attributed solely to the nucleic acid and its structural changes. As shown in Figure 5, the native B-form pDNA has a characteristic spectrum with an ellipticity maximum at 274 nm and a minimum at 248 nm due to $\pi \rightarrow \pi^*$ transitions of the purine and pyrimidine bases.[26−28] In general, as polymer binds to pDNA from N/P = 0 to 5, there is a red shift in the positive peak and a loss of its rotational strength (Figure 5), two changes formerly ascribed to the transition from B- to C-form secondary structure.[29] Although these spectral changes are now thought to reflect simply modification of the B-form DNA, they do indicate that polymer binding increases the separation and tilt angle of the base pairs relative to the helix axis,[29] suggesting direct interaction between the PAAs and nucleic acid. These characteristics are more pronounced in the case of **A4**, even at an N/P as low as 0.5. With polymer **S4**, the CD spectrum of pDNA shifts at N/P = 2, and with **O4**, this shift occurred at a slightly higher N/P ratio. These data support the ITC results that also show that the order of pDNA binding affinity is **A4** > **S4** > **O4**. Therefore, we conclude that the longer methylene spacer in the repeat unit of **A4** may provide a slightly enhanced pDNA binding capability through hydrogen bonding to the backbone or bases, through optimal electrostatic interaction, or, more likely, through a combination of both events. The different linker lengths between the amides and amines could help to strengthen these interactions.

Hydrophobic Contribution to the Interaction Between the PAAs and pDNA. One of the driving forces of polymer binding to pDNA could be hydrophobic in nature. The hydrophobic effect is common in protein−nucleic acid and enzyme−substrate interactions and refers to the burial of nonpolar regions of macromolecules to minimize exposure to polar solvents, in particular water. Acyl chains in cationic lipids have been previously shown to enable DNA binding cooperativity via the hydrophobic effect, and, in fact, each methylene

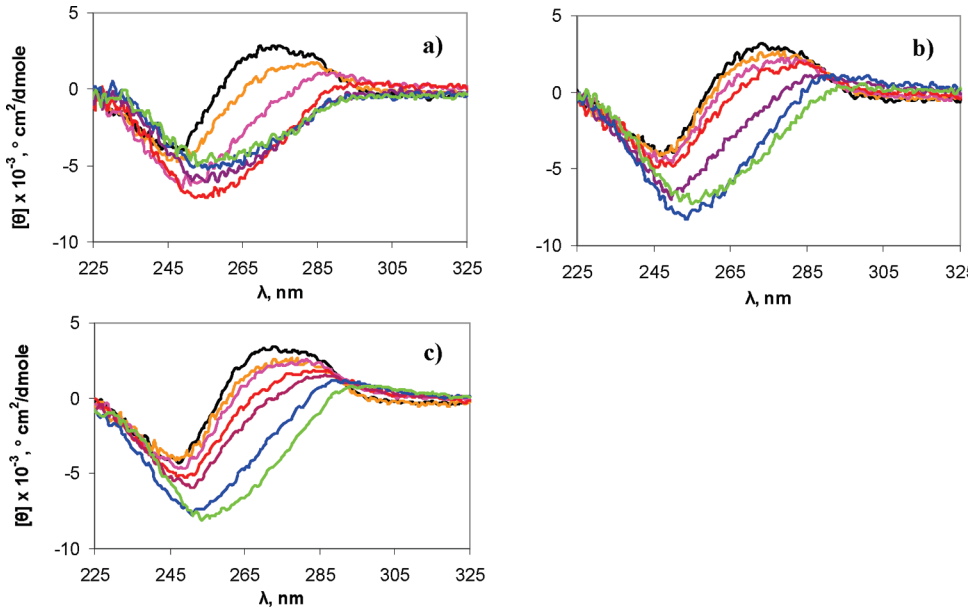

Figure 5. CD spectra of 5.5 mM (a) **A4**, (b) **S4**, and (c) **O4** titrated into 0.31 mM pDNA in 10 mM Tris pH 7.4 buffer at N/P ratio = 0 (black), 0.5 (orange), 1.0 (pink), 1.5 (red), 2.0 (purple), 3.0 (blue), 5.0 (green).

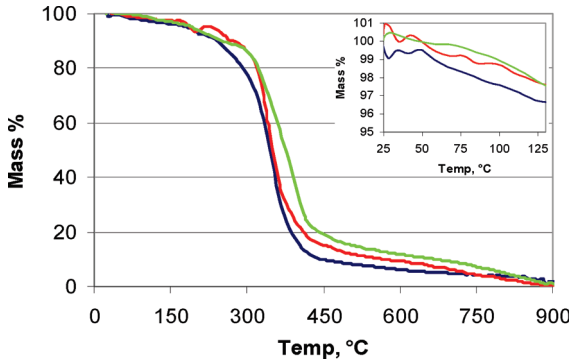

Figure 6. Thermal gravimetric analysis of **A4** (red), **S4** (green), and **O4** (blue). The inset shows the mass loss due to water evaporation from 0 to 125 °C.

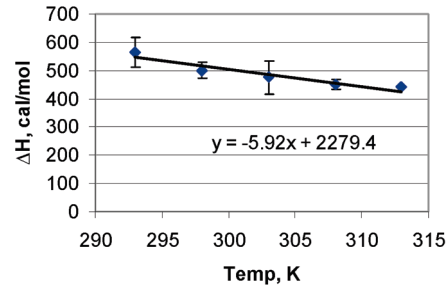

Figure 7. Change in ΔH of **A4**-pDNA binding in 10 mM Tris pH 7.4 buffer with increasing temperature, as determined by microcalorimetry. The slope of the best-fit line provides the magnitude of the heat capacity.

group adds four-fold to the DNA binding affinity.[30,31] Of equal importance to this mechanistic study is the study of DNA condensation by Vijayanathan et al. using structurally similar polyamines. Static and dynamic light scattering experiments on spermine homologues of varying methylene bridge size (from 2−12) revealed that the length of this region has a profound effect on the ability to condense DNA and the size of the condensate.[32] In light of all of these previous conclusions, understanding the role of the hydrophobic effect in the binding of our PAAs to pDNA, especially in comparison to our PGAAs lacking the methylene spacers, is crucial to a complete understanding of their binding mechanisms.

The different lengths of methylene spacer present in the repeat units of these PAAs allow the possibility of varying hydrophobicity of the chains. Because the level of polymer hydration could also present another variable into the thermodynamic parameters of their pDNA association, it is important to determine if this factor changes with the spacer from **A4** to **S4** to **O4**. For this comparison, we used thermal gravimetric analysis. A sample of each polymer was heated from 25 to 900 °C, and the percent of polymer mass loss was measured as a function of temperature (Figure 6). We noticed a steady decrease in polymer mass between 25 and 300 °C, which we mostly attribute to the loss of water. Significant polymer decomposition was noticed at a temperature of ∼300 °C, as evidenced by the sharp decrease in mass percent. As shown in the inset of Figure 6, the hydration states of **A4**, **S4**, and **O4** are similar, yet **O4** was demonstrated to be slightly more hydrophilic (higher mass loss of water). Polymer **A4** does bind pDNA with the highest strength of the series; however, **O4** yields the highest gene expression,[8] which is possibly due to the degradation of the structure.

The heat capacity (ΔC_p) of a system is considered to arise solely from changes in solvation,[33−35] and thus measuring the heat capacity of polycations upon pDNA association is a logical experiment to further examine the role of methylene length (and slight changes in hydrophilicity) of these PAAs in pDNA affinity. Under experimental conditions similar to those of the previous ITC studies herein, enthalpies at increasing temperature were used to obtain the ΔC_p value. Polymer **A4**, which revealed the strongest pDNA association and slightly lower hydration, was chosen as a model system for the ΔC_p study to understand the extent, if any, of hydrophobic interaction (Figure 7). The magnitude of the heat capacity for **A4**-pDNA binding (−5.9 cal/(mol K)) was smaller than expected for the occurrence of hydrophobic interactions. Burial of a methylene group should account for a heat capacity of −13.5 cal/(mol K), and this number can be directly attributed to the number of buried methylenes in a lipid chain.[36] Because the least hydrated polymer, **A4**, presented such a weak thermodynamic contribution from solvation changes, we have evidence leading to the conclusion that hydrophobic interactions do not play a substan-

tial role in the binding mechanisms of the three PAAs. This was also shown to be the case for spermine−DNA binding.[20] The discovery that hydrophobic interactions are not contributing substantially to the binding between DNA and polymers with methylene spacers, whereas they are important in DNA−lipid complexes, may be expected considering the differences in structure. Acyl chains in a lipid tail are free to adopt a conformation favoring hydrophobic associations, unlike the short, restricted monomers in both our polymers and the spermine molecule. Therefore, charge−charge, hydrogen bonding, and van der Waals appear to be the dominant forces present in the binding of these polymeric agents to pDNA.

One possible reason for the differences in pDNA affinity and extent of hydrogen bonding interaction present among these three similar PAAs is the spacing between the amide linkages. Kopka et al. discovered that DNA binding of the antibiotic netropsin occurred through hydrogen bond formation between the drug amides and exposed adenine N-3 and thymine O-2 on the floor of the minor groove.[37] Schultz and Dervan also showed that increasing the length of netropsin and distamycin analogs could enable their binding of other sequences of double-stranded DNA.[38] Applying this reasoning to our system, the increased spacer length could possibly explain the increasing pDNA binding strength we have shown from **O4** < **S4** < **A4**.

Conclusions

Understanding the mechanism of nucleic acid interaction of polymeric vectors is crucial to the intelligent design of more efficacious agents. Previously, we designed and synthesized a series of glycopolymers called the PGAAs. These systems have demonstrated strong pDNA binding, efficient transfection ability in several mammalian cell lines, low cytotoxicity, and the ability to degrade under aqueous conditions. Here we studied an analogous polymer series that lacks the carbohydrate hydroxyl moieties (and exhibits different degradation and biological properties) to investigate the physiochemical differences in pDNA binding. On the basis of the quantitative microcalorimetry data, we have shown that the pDNA affinity increases slightly with the length of the methylene spacer in the repeat unit of the polymer. This conclusion was substantiated by the circular dichroism spectra, which suggested enhanced base pair interaction with longer spacer length as well, possibly due to hydrogen bond formation from the amide groups.

In this study, we evidence that hydrophobic interactions do not substantially contribute to the binding mechanism with these PAA structures. The association is therefore attributed to a combination of electrostatic, van der Waals, and hydrogen bonding forces, which could be strengthened by increasing the distance between the amide monomer linkers. Using the conclusions attained herein, we have a better understanding of the structural features necessary for efficient pDNA binding, and we know that the carbohydrate hydroxyl groups contained in the PGGAs are not necessary for binding and compaction but can enhance the binding strength, depending on their stereochemistry. In addition, whereas enhanced binding affinity appears to be a factor in efficient transfection of polyplexes formed with these structures, gene expression also appears to be driven by the degradation of the polymeric vehicle. The characterization tools and structure−property studies utilized and performed herein are important to the area of polymeric nucleic acid delivery vehicle development to understand and optimize the factors dictating delivery efficacy.

Acknowledgment. We thank Dr. Yemin Liu and Lisa Bartholomew for synthesizing the polymers used in these studies. We also thank Professor Apryll Stalcup (University of Cincinnati) for the use of her CD spectrometer. This work was supported by The National Science Foundation CAREER Award program (CHE-0449774). T.M.R. acknowledges support by the Alfred P. Sloan Research Fellow program.

References and Notes

(1) Godbey, W. T.; Wu, K. K.; Mikos, A. G. *J. Biomed. Mater. Res.* **1999**, *45*, 268–275.
(2) Liu, Y.; Wenning, L.; Lynch, M.; Reineke, T. M. *J. Am. Chem. Soc.* **2004**, *126*, 7422–7423.
(3) Srinivasachari, S.; Liu, Y.; Zhang, G.; Prevette, L.; Reineke, T. M. *J. Am. Chem. Soc.* **2006**, *128*, 8176–8184.
(4) Davis, M. E.; Pun, S. H.; Bellocq, N. C.; Reineke, T. M.; Popielarski, S. R.; Mishra, S.; Heidel, J. D. *Curr. Med. Chem.* **2004**, *11*, 179–197.
(5) Liu, Y.; Reineke, T. M. *J. Am. Chem. Soc.* **2005**, *127*, 3004–3015.
(6) Liu, Y.; Reineke, T. M. *Bioconjugate Chem.* **2006**, *17*, 101–108.
(7) Prevette, L. E.; Kodger, T. E.; Reineke, T. M.; Lynch, M. L. *Langmuir* **2007**, *23*, 9773–9784.
(8) Liu, Y.; Reineke, T. M. *Biomacromolecules* **2010**, DOI: 10.1021/bm9008233.
(9) Kielkopf, C. L.; Baird, E. E.; Dervan, P. B.; Rees, D. C. *Nat. Struct. Biol.* **1998**, *5*, 104–109.
(10) Dervan, P. B.; Edelson, B. S. *Curr. Opin. Struct. Biol.* **2003**, *13*, 284–299.
(11) Pilch, D. S.; Poklar, N.; Baird, E. E.; Dervan, P. B.; Breslauer, K. J. *Biochemistry* **1999**, *38*, 2143–2151.
(12) Read, M. L.; Bettinger, T.; Oupicky, D. In *Nonviral Vectors for Gene Therapy*; Findeis, M. A., Ed.; Humana Press: Totowa, NJ, 2001; Vol. 65, pp 131−148.
(13) Lyubchenko, Y. L.; Shlyakhtenko, L. S. *Proc. Natl. Acad. Sci. U.S.A.* **1997**, *94*, 496–501.
(14) Boles, T. C.; White, J. H.; Cozzarelli, N. R. *J. Mol. Biol.* **1990**, *213*, 931–951.
(15) Wiseman, T.; Williston, S.; Brandts, J. F.; Lin, L.-N. *Anal. Biochem.* **1989**, *179*, 131–137.
(16) Prevette, L. E.; Lynch, M. L.; Kizjakina, K.; Reineke, T. M. *Langmuir* **2008**, *24*, 8090–8101.
(17) Srinivasachari, S.; Liu, Y.; Prevette, L.; Reineke, T. M. *Biomaterials* **2007**, *28*, 2885–2898.
(18) Alvarez-Lorenzo, C.; Barreiro-Iglesias, R.; Concheiro, A.; Iourtchenko, L.; Alakhov, V.; Bromberg, L.; Temchenko, M.; Deshmukh, S.; Hatton, T. A. *Langmuir* **2005**, *21*, 5142–5148.
(19) Matulis, D.; Rouzina, I.; Bloomfield, V. A. *J. Mol. Biol.* **2000**, *296*, 1053–1063.
(20) Patel, M. M.; Anchordoquy, T. J. *Biophys. J.* **2005**, *88*, 2089–2103.
(21) Lobo, B. A.; Davis, A.; Koe, G.; Smith, J. G.; Middaugh, C. R. *Arch. Biochem. Biophys.* **2001**, *386*, 95–105.
(22) Record, M. T. J.; Ha, J. H.; Fisher, M. A. *Methods Enzymol.* **1991**, *208*, 291–343.
(23) Nisha, C. K.; Manorama, S. V.; Ganguli, M.; Maiti, S.; Kizhakkedathu, J. N. *Langmuir* **2004**, *20*, 2386–2396.
(24) Zhou, Y.-L.; Li, Y.-Z. *Spectrochim. Acta, Part A* **2004**, *60*, 377–384.
(25) Kennedy, M.; Pozharski, E.; Rakhmanova, V.; MacDonald, R. *Biophys. J.* **2000**, *78*, 1620–1633.
(26) Bloomfield, V. A.; Crothers, D. M.; Tinoco, I. *Physical Chemistry of Nucleic Acids*; Harper & Row Publishers: New York, 1974.
(27) Gray, D. M.; Ratliff, R. L.; Vaughan, M. R. In *Spectroscopic Methods for Analysis of DNA*; Academic Press: New York, 1992; Vol. 211, pp 389−397.
(28) Rodger, A.; Norden, B. *Circular Dichroism and Linear Dichroism*; Oxford University Press: Oxford, U.K., 1997.
(29) Tunis-Schneider, M. J. B.; Maestre, M. F. *J. Mol. Biol.* **1970**, *52*, 521–541.
(30) Spink, C. H.; Chaires, J. B. *J. Am. Chem. Soc.* **1997**, *119*, 10920–10928.
(31) Matulis, D.; Rouzina, I.; Bloomfield, V. A. *J. Am. Chem. Soc.* **2002**, *124*, 7331–7342.
(32) Vijayanathan, V.; Thomas, T.; Shirahata, A.; Thomas, T. J. *Biochemistry* **2001**, *40*, 13644–13651.
(33) Baldwin, R. L. *Proc. Natl. Acad. Sci. U.S.A.* **1986**, *83*, 8069–8072.
(34) Murphy, K. P.; Gill, S. J. *Thermochim. Acta* **1990**, *172*, 11–20.
(35) Spolar, R. S.; Livingstone, J. R.; Record, M. T. J. *Biochemistry* **1992**, *31*, 3947–3955.
(36) Heerklotz, H.; Epand, R. M. *Biophys. J.* **2001**, *80*, 271–279.
(37) Kopka, M. L.; Yoon, C.; Goodsell, D.; Pjura, P.; Dickerson, R. E. *Proc. Natl. Acad. Sci. U.S.A.* **1985**, *82*, 1376–1380.
(38) Schultz, P. G.; Dervan, P. B. *J. Biomol. Struct. Dyn.* **1984**, *1*, 1133–1147.

BM900824G